(19) Europäisches Patentamt
European Patent Office
Office européen des brevets

(11) EP 3 055 644 B1

(12) **EUROPEAN PATENT SPECIFICATION**

(45) Date of publication and mention of the grant of the patent:
29.05.2019 Bulletin 2019/22

(21) Application number: **14851972.1**

(22) Date of filing: **13.10.2014**

(51) Int Cl.:
G01B 11/00 *(2006.01)* ***G01J 3/28*** *(2006.01)*
A61B 5/00 *(2006.01)* ***G01N 21/47*** *(2006.01)*

(86) International application number:
PCT/CN2014/088517

(87) International publication number:
WO 2015/051767 (16.04.2015 Gazette 2015/15)

(54) **WAVELENGTH-ENCODED TOMOGRAPHY**

WELLENLÄNGENCODIERTE TOMOGRAFIE

TOMOGRAPHIE CODÉE EN LONGUEUR D'ONDES

(84) Designated Contracting States:
AL AT BE BG CH CY CZ DE DK EE ES FI FR GB GR HR HU IE IS IT LI LT LU LV MC MK MT NL NO PL PT RO RS SE SI SK SM TR

(30) Priority: **11.10.2013 US 201361890048 P**

(43) Date of publication of application:
17.08.2016 Bulletin 2016/33

(73) Proprietor: **The University of Hong Kong**
Hong Kong (CN)

(72) Inventors:
- **WONG, Kin Yip, Kenneth**
  Hong Kong (CN)
- **ZHANG, Chi**
  Hong Kong (CN)

(74) Representative: **HGF Limited**
8th Floor
140 London Wall
London EC2Y 5DN (GB)

(56) References cited:
EP-A1- 1 870 030
CN-A- 103 284 691
CN-A- 103 284 691
US-A1- 2003 025 913
US-A1- 2004 136 577
US-A1- 2012 127 476

- **ONUR KUZUCU ET AL: "Spectral phase conjugation via temporal imaging", OPTICS EXPRESS, vol. 17, no. 22, 26 October 2009 (2009-10-26), page 20605, XP055365788, ISSN: 2161-2072, DOI: 10.1364/OE.17.020605**
- **REZA SALEM ET AL: "Application of space-time duality to ultrahigh-speed optical signal processing", ADVANCES IN OPTICS AND PHOTONICS, vol. 5, no. 3, 30 September 2013 (2013-09-30), page 274, XP055365768, ISSN: 1943-8206, DOI: 10.1364/AOP.5.000274**
- **MOTI FRIDMAN ET AL: "Demonstration of temporal cloaking", NATURE, vol. 481, no. 7379, 5 January 2012 (2012-01-05), pages 62-65, XP055015746, ISSN: 0028-0836, DOI: 10.1038/nature10695**
- **CHI ZHANG ET AL: "Parametric spectro-temporal analyzer (PASTA) for real-time optical spectrum observation", SCIENTIFIC REPORTS, vol. 3, 24 June 2013 (2013-06-24), XP055365561, DOI: 10.1038/srep02064**
- **BENNETT C V ET AL: "Principles of parametric temporal imaging. I. System configurations", IEEE JOURNAL OF QUANTUM ELECTRONICS, IEEE SERVICE CENTER, PISCATAWAY, NJ, USA, vol. 36, no. 4, 4 April 2000 (2000-04-04), pages 430-437, XP011449678, ISSN: 0018-9197, DOI: 10.1109/3.831018**
- **LI, QIAN ET AL.: 'Control of Optical Rogue Waves in Supercontinuum Generation with a Minute Continuous Wave.' OPTICAL SOCIETY OF AMERICA 31 December 2011, XP031892139**

Printed by Jouve, 75001 PARIS (FR)

(Cont. next page)

- **ZHU, RUI ET AL.: 'Dual-Band Time-Multiplexing Swept-Source Optical Coherence Tomography Based on Optical Parametric Amplification.' IEEE JOURNAL OF SELECTED TOPICS IN QUANTUM ELECTRONICS vol. 18, no. 4, 06 July 2012, pages 1287 - 1292, XP011455354**

Description

BACKGROUND OF THE INVENTION

[0001] Medical imaging can include capturing images of biological structures by using, for example, Computer Aided Tomographic (CAT) scanning, and can be a highly beneficial biophotonic measuring technique. A biophotonic system, which may be useful for, e.g., cardiovascular medical applications may comprise a tomographic imaging device and one or more endoscopic instruments. Biophotonic applications may also include dermatological (e.g., skin tissue) examinations and/or imaging of dental structures.

[0002] Tomographic imaging technologies, such as the computed tomography by x-ray, magnetic resonance imaging (MRI), ultrasound imaging, and optical coherence tomography (OCT) have found widespread applications in micro-scale bio-medical imaging. Among these technologies, OCT is advantageous in terms of resolution, owing to its short wavelength. Optical frequencies are beyond the detectable range of electrical means, and OCT systems leverage the low frequency introduced by an interferometer to differentiate reflective depth. In addition, some straightforward methods like radio detection and ranging (RADAR) or optical time domain reflectometers (OTDR) can only measure large-scale distances, and the resolution is limited by the bandwidth of the oscilloscope.

[0003] OCT has proven to be useful in medical and laboratory environments at least in part due to a capability for resolving fine structures in a non-invasive manner. OCT may be useful, for example, in performing optical biopsies, which can permit a physician or other medical professional to perform noninvasive *in vivo* imaging without a need for slicing tissue samples. OCT can also allow for imaging of highly scattered biological tissues with a high resolution.

[0004] ONUR KUZUCU ET AL, "Spectral phase conjugation via temporal imaging", OPTICS EXPRESS, (20091026) discloses spectral phase conjugation via temporal imaging. REZA SALEM ET AL, "Application of space-time duality to ultrahigh-speed optical signal processing", ADVANCES IN OPTICS AND PHOTONICS, (20130930) discloses an application of space-time duality to ultrahigh-speed optical signal processing. MOTI FRIDMAN ET AL, "Demonstration of temporal cloaking", NATURE, (20120105) discloses a demonstration of temporal cloaking. CHI ZHANG ET AL, "Parametric spectro-temporal analyzer (PASTA) for real-time optical spectrum observation", SCIENTIFIC REPORTS, (20130624) discloses a parametric spectro-temporal analyzer (PASTA) for real-time optical spectrum observation. BENNETT C V ET AL, "Principles of parametric temporal imaging. I. System configurations", IEEE JOURNAL OF QUANTUM ELECTRONICS, IEEE SERVICE CENTER, PISCATAWAY, NJ, USA, (20000404) discloses principles of parametric temporal imaging. CN 103 284 691 A discloses a method and apparatus for performing optical imaging using frequency-domain interferometry.

BRIEF SUMMARY OF THE INVENTION

[0005] The invention is set out in the claims. Embodiments of the subject invention provide advantageous systems and methods for non-invasive optical imaging (e.g., non-invasive, optical, cross-sectional imaging), which have a wide range of uses and are particularly beneficial in biological systems. In disclosed examples, a wavelength-encoded tomography system can utilize one or more time-lenses to perform an optical Fourier transform, and the time-to-wavelength conversion can generate a wavelength-encoded image of optical scattering from internal microstructures (e.g., analogous to interferometery-based imaging such as optical coherence tomography). Optical Fourier transform, provides better axial resolution than electrical Fourier transform and greatly simplifies the digital signal processing after data acquisition.

[0006] In an example, an imaging system can include: a sample platform; a photodetector; a linear frequency-shifted device positioned such that light from the sample passes through the linear frequency-shifted device before it reaches the photodetector; and a processing device in operable communication with the photodetector and configured to receive an output spectrum from the photodetector and realize a spatial-to-wavelength conversion, of the output spectrum, solely in the optical domain. The linear frequency-shifted device can include one or more time-lenses. The system can be capable of achieving an imaging resolution of 150 μm or less with a spectral width of 7.5 nm, and an A-scan rate of at least 100 MHz.

[0007] In another example, a method for imaging a sample can include: placing the sample on a sample platform of an imaging system; positioning a linear frequency-shifted device such that light from the sample passes through the linear frequency-shifted device before it reaches a photodetector of the imaging system; receiving, by a processing device in operable communication with the photodetector, an output spectrum from the photodetector; and realizing, by the processing device, a spatial-to-wavelength conversion, of the output spectrum, solely in the optical domain. The linear frequency-shifted device can include one or more time-lenses. The method can achieve an imaging resolution of 150 μm or less with a spectral width of 7.5 nm, and an A- scan rate of at least 100 MHz.

BRIEF DESCRIPTION OF THE DRAWINGS

[0008]

Figure 1(a) shows a schematic of the principle of depth-to-wavelength conversion in the spatial domain by a system according to an example.
Figure 1(b) shows a schematic of the principle of depth-to-wavelength conversion in the spatial domain by a system according to an example.
Figure 1(c) shows a schematic of the principle of depth-to-wavelength conversion in the temporal domain by a system according to an example.
Figure 1(d) shows a schematic of the principle of depth-to-wavelength conversion in the temporal domain by a system according to an example.
Figure 2 shows a schematic of an imaging system according to an example.
Figure 3(a) shows a spectrum of mixing in a system according to an example.
Figure 3(b) shows a spectrum of mixing in a system according to an example.
Figure 4 shows a plot of intensity versus wavelength for characterization of depth-to-wavelength conversion by a system according to an example.
Figure 5 shows a schematic of an imaging system according to an example.
Figure 6 shows a schematic of an imaging system according to an example.
Figure 7 shows a schematic of an imaging system according to an example.

DETAILED DISCLOSURE OF THE INVENTION

[0009] Embodiments of the subject invention provide advantageous systems and methods for non- invasive optical imaging (e.g., non-invasive, optical, cross-sectional imaging), which have a wide range of uses and are particularly beneficial in biological systems. A wavelength-encoded tomography system can utilize one or more time-lenses to perform an optical Fourier transform, and the time-to-wavelength conversion can generate a wavelength-encoded image of optical scattering from internal microstructures (e.g., analogous to interferometery-based imaging such as optical coherence tomography). Optical Fourier transform, provides better axial resolution than electrical Fourier transform and greatly simplifies digital signal processing after data acquisition.

[0010] In an example, an optical imaging system can capture tomographic (layer) images in a non-invasive manner and enable ultrafast frame rate with high resolution and sensitivity. The system can include one or more of the following elements: means for introducing a linear frequency shifted device (e.g., a time-lens) in front of a sample being imaged (e.g., between the sample platform and a photodetector of the system); means for differentiating the depth induced delay when the light transmits forward and backward through the system, as the spectrum is stretched and compressed; means for illuminating light on the sample by a swept-source, as different reflecting depth results in different output wavelengths after the compression process, thereby realizing the identification of different layers; and means (e.g., a processing device such as a processor of a computing device, or an optical spectrum analyzer) for realizing the spatial to wavelength conversion all in the optical domain without pursuing mandatory electrical Fourier transformation (as in OCT). All components can be in operable communication with each other (e.g., via wires, wirelessly, or a combination of both). The system can be configured for: realizing the all-optical spatial to wavelength conversion, with flexible conversion factor for different applications; providing orders of magnitude improvement on the frame rate, as high as megahertz or even gigahertz, compared with the related art OCT systems; or both.

[0011] Existing tomographic imaging technologies have limitations with regard to resolution, depth, and frequency. To help address these limitations, an ultrafast optical oscilloscope incorporating a time-lens approach can be used. A short pulse of 200 femtoseconds (fs) can be resolved in the spectral domain. The combination of two schemes (OTDR and the time-lens oscilloscope) can directly convert a tiny depth difference into a wavelength shift, thereby providing an advantageous solution for advanced ultrafast tomographic applications; such a solution is referred to herein as wavelength-encoded tomography (WET). This technique overcomes inherent speed limitation of OCT, while also improving the resolution in non-invasive cross-sectional imaging.

[0012] It is possible that the femtosecond pulse used by the time-lens oscilloscope may encounter undesirable nonlinear effects in biological samples, which would affect the imaging quality of a linear scattering system (e.g., OCT). Therefore, in many embodiments of the subject invention, the single time-lens focusing structure can be adjusted to two time-lenses, with opposite focal group-dispersion delays (GDDs) to avoid the ultra-short pulse interacting with the sample. Figure 1 shows a temporal ray diagram of a WET configuration according to an embodiment, which can be understood by the space-time duality.

[0013] Referring to Figure 1, the spatial distance (d) along the vertical axis corresponds to the temporal delay (Δt), and the spatial axial angle (θ) corresponds to the temporal wavelength ($\Delta\lambda$). In Figure 1(a), one converging lens and

one diverging lens with identical focal lengths (f) are aligned with each other, and tilting of the axial angle ($\theta = d/f$) is achieved by the offset (d) between these two lenses along the vertical axis (Figure 1(b)). Therefore, in the temporal domain, these two corresponding time-lenses can realize linear optical mapping between the reflective temporal delay ($\Delta t = 2d/c$) and the wavelength ($\Delta\lambda$). In addition, no short pulse is involved throughout this process, and the energy is distributed uniformly along the time span.

[0014] In an embodiment, two time-lenses are implemented with a swept-pumped four-wave mixing (FWM) process (Figures 1(c) and 1(d)), owing to the required large swept bandwidth and less than gigahertz frame rate. The identical focal GDDs (Φ_f) are achieved with the same swept-pump, while the converging and diverging features are realized with different parametric mixing directions, from short wavelength to long wavelength and vice versa. After time-lens 1, the newly generated idler can be launched to illuminate a reflective sample, which can scatter the idler along the temporal axis before combining together with the same swept-pump in time-lens 2. In certain embodiments, time-lens 2 generates a quasi-CW (where CW refers to continuous wave) source as the input signal, and the delayed idler changes its wavelength, represented by the dashed and dotted lines shown in Figure 1(d). This mechanism provides a linear relation between the reflection depth (d) and the output wavelength shift ($\Delta\lambda$) as follows:

$$\Delta\lambda = \frac{\lambda_0^2}{2\pi c}\cdot\frac{\Delta f}{\Phi_f} = \frac{4}{cDL}d = \varepsilon\cdot d, \qquad (1)$$

where c is the speed of light, DL is the swept-pump dispersion (which can be generated from, e.g., a stretched pulse), and $\varepsilon = 4/cDL$ is the depth-to-wavelength ratio. The detailed derivation of ε can be obtained from Figure 1(d) and Zhang et al. (Appl. Opt. 52, 8817-8826, 2013).

[0015] Figure 2 shows a schematic of an imaging apparatus according to an embodiment of the subject invention. Though certain values are shown in Figure 2, these are for exemplary purposes only and should not be construed as limiting. Referring to Figure 2, a setup including two time-lenses is shown. A pulsed source (e.g., 500-fs pulsewidth, λ_{BW} = 7.5 nm) can pass through a spool of fiber (e.g., 1-km single-mode fiber, such as SMF-28, DL = 17 picoseconds/nanometer (ps/nm)) to generate the swept-pump for the two-stage FWMs. The FWM can leverage the third-order nonlinear susceptibility χ in two spools of fibers (e.g., 50-m highly-nonlinear dispersion-shifted fibers (HNL-DSFs)). The zero-dispersion wavelength can be at, for example, 1554 nm, though embodiments are not limited thereto. In the first-stage FWM (the left shaded box in Figure 2), a signal **S1** (e.g., a 1-mW CW signal) and the swept-pump (which can be amplified, e.g., to 100 milliwatts (mW)) generate the idler (**I1**) with doubled swept range. The doubled swept range is shown in Figure 3(a). The idler (**I1**) can have a value of, e.g., 0.5 mW, though embodiments are not limited thereto. The idler (**I1**) can be filtered out by a wavelength-division multiplexing (WDM) filter and amplified (e.g., to 10 times its initial value such as to 5 mW) by an amplifier before illuminating the sample. In a particular embodiment, the amplifier can be an L-band Erbium doped fiber amplifier (EDFA).

[0016] The sample arm (or sample platform) can introduce some loss (e.g., ~10-dB loss), and different reflection depths can scatter the idler (**I1**) with corresponding temporal delays. An optical delay line in the sample arm can synchronizes the scattered idlers (**S2**, as the signal for the second-stage FWM) with the second swept-pump. Therefore, after the second-stage FWM, the idler (**I2**) is generated at the original signal wavelength, and this is depicted in Figure 3(b). The idler (**I2**) can have a value of, e.g., ~0.2 mW, though embodiments are not limited thereto. The idler (**I2**) spectrum can be captured by a processing device, such as an optical spectrum analyzer (for example, OSA, Yokogawa AQ6370C, 0.05-nm resolution) and can manifest the spatial information (A_0, A_1, and A_2 in the sample arm of Figure 2). The spatial information is shown as the output spectra (λ_0, λ_1, and λ_2) of Figure 2. Moreover, the two time-lenses configuration can employ a CW source as the signal, and in this case no synchronization is required between the signal and pulsed pump, unlike related art imaging devices. The overall setup can be pictorially viewed as a "lock" system: the FWM1 can lock a swept-pump onto the CW signal, and the FWM2 using the same swept-pump as a "key" to unlock the temporal delay (i.e., reflection depth information) from the wavelength shifting.

[0017] According to Equation (1), the output wavelength shift ($\Delta\lambda$) is directly proportional to the reflection depth (d). To quantitatively characterize this feature, a precision translation stage can be introduced to control the reflective mirror. In the WET system according to certain embodiments of the subject invention, the spatial resolution (R_{WET}) refers to the capability of an optical imaging system to distinguish different layers, which can be calculated with the spectral width ($\delta\lambda$) and the mapping ratio (ε). The ideal $\delta\lambda$ can be determined by the temporal pulsewidth ($\lambda_{BW}DL$), which can be narrowed by the FWM process. Frequency intensity fluctuation of the swept-pump may limit $\delta\lambda$. If there is no intensity fluctuation over the envelope of the swept-pump, and phase-matching condition is satisfied over the whole conversion

range, then the spatial resolution of the WET system can be shown as

$$R_{WET} = \delta\lambda/\varepsilon = \lambda_0^2/(2\pi c) \times 4\ln 2/(\lambda_{BW} DL) \times cDL/4 = \ln 2\lambda_0^2/(2\pi\lambda_{BW}), \quad (2)$$

where λ_{BW} is the full-width at half-maximum (FWHM) of the swept-pump spectrum. Based on the pump bandwidth (λ_{BW}), the ideal spatial resolution can be calculated. Compared with OCT, system of the subject invention can achieve four times sharper resolution with the same bandwidth (λ_{BW}) based on Equation (2). The doubled frequency relation from the swept-pump to the idler in the FWM (i.e., the idler bandwidth can be doubled of the pump) contributes a factor of two, and the optical Fourier transform (i.e., WET) achieves better temporal resolution over the digital (electrical) Fourier transform (i.e., OCT) by another factor of two. Specifically, the optical Fourier transform by the time-lens has taken into account the phase term, while the electrical Fourier transform in OCT is performed after the square-law photodetector, which only considers the intensity part. The second factor of two is guaranteed, while the first factor (conversion bandwidth) could potentially be limited in certain circumstances by the phase-matching condition of the FWM

[0018] Figures 3(a) and 3(b) show the spectra of two-stage FWMs. The conversion bandwidth can also limit the resolution in certain circumstances, and the phase matching condition can require shorter HNL-DSF with lower dispersion coefficient (D) and slope (S). Some advanced dispersion-engineered nonlinear medium, such as a silicon waveguide, can help to achieve 100-nm FWM wavelength conversion bandwidth, which can benefit the implementation of a WET system according to embodiments of the subject invention. The inset of Figure 3(b) shows a comparison between the input and the output spectra, which is broadened. Two factors can contribute to this spectral broadening effect: the phase-mismatching can decrease the pulsewidth of idler (**I1**) by 30%, since its bandwidth is degraded after FWM1 (as shown in Figure 3(a)); and the temporal intensity fluctuation of the swept-pump can introduce another factor of two to the spectral width of the idler (**I2**). Considering the same narrowing effect in FWM2, the pulsewidth of idler (**I2**) can decrease by half, thereby broadening the spectral width by a factor of two. Figure 5 shows an imaging apparatus according to an embodiment of the subject invention. To capture a 2D cross-sectional image, a galvo mirror (**M1**) can be used to scan in the sample arm as shown in the top box of Figure 5. The apparatus having two time-lenses can optically convert the depth information to spectrum, and the spectrum can be captured to construct the 2D image. In this sense, it is similar to spectral-domain OCT (SD-OCT), which also requires a spectrometer to capture the spectral information. However, the spectrum in SD-OCT carries interference fringes, and further Fourier transform is required to retrieve the depth information. In a WET system/apparatus according to the subject invention, the spectrum can directly generate the depth information (with better resolution compared to SD-OCT), for example, by being captured by a synchronized single-shot spectrometer. The system can therefore be configured as an ultrafast tomographic system.

[0019] To fully utilize the high frame rate (e.g., 100-MHz frame rate) of the systems of the subject invention, two methods can be used. In one such method, the spectrum can be dispersed onto a spatial CCD sensor (Figure 5(a)) and another scanning galvo mirror (**M2**) can be combined along the horizontal direction to construct the 2D image. Mirrors **M1** and **M2** can be synchronized by the identical driving signal, and the B-scan rate can be determined by the frame rate of the CCD sensor (as high as ~kHz). In another such method, an ultrafast optical spectrum analyzer can be utilized - a parametric spectro-temporal analyzer (PASTA), with high resolution (e.g., 0.02-nm resolution). The PASTA system can share the same pump source with the WET system, which naturally synchronizes these two systems together, therefore fully utilizing the 100-MHz A-scan rate, as shown in Figure 5(b).

[0020] A time domain OCT (TD-OCT) approach is sometimes employed for rapid image capture. TD-OCT can include a Michelson-type interferometer and focused sample arm beam arranged in a lateral-scanning mechanism. Another approach toward improving noninvasive medical imaging can include "single-shot" imaging, in which a large amount of imaging measurements can be performed in a very short period of time. Single-shot imaging can benefit from enhanced OCT imaging speed which may achieved at least in part through use of, for example, frequency domain optical coherence tomography (FD-OCT). In FD-OCT, axial (e.g., axial line, A-line, etc.) back-reflection signals in a frequency domain can be exploited, which can equate to, for example, a wave-number domain.

[0021] In embodiments of the subject invention, WET can provide advantages over TD-OCT and FT-OCT. For example, embodiments can reduce or eliminate a need for a reference branch, which may be used to bring about, for example, an interference pattern between direct and scattered imaging beams generated in OCT systems. Thus, if a reference branch is not utilized (i.e., excluded), optical components that may introduce data capture speed limitations, such as a Mach Zehnder interferometer for capturing phase shifts at locations within an interference pattern, may be eliminated. Additionally, an all-optical process can be used, in which the output signal intensity from optical components directly reflects the spatial information. Accordingly, in certain embodiments, post processing, which can sometimes be performed after optical signals are converted to electrical signals, need not be performed. At least as a partial consequence of eliminating or reducing the need for electronic post processing, a WET system may bring about considerable, (e.g., a tenfold or more) increase in frame rate. Improvements can enable capture of as many as, e.g., 1,000,000 or 1,000,000,000

frames per second, though embodiments are not limited thereto. An additional benefit can be a reduction in system complexity over TD-OCT and/or FD-OCT approaches.

[0022] Referring again to Figures 1(c) and 1(d), in an embodiment, a WET system can leverage time-sensitive features of a linear frequency shifting device (time-lens) to differentiate spatial depth induced delay. A principal portion of a WET system can include a spatial depth-to-wavelength conversion. A two-stage, four-wave mixing (FWM1) element can be employed. A first stage can use a swept-pump ("lock") signal and a CW signal to generate optical signals corresponding to a double-chirped idler to illuminate a sample undergoing imaging. In embodiments, responsive to illumination, different layers of a sample undergoing imaging may scatter or reflect an idler signal at different times. Scattered idlers may be combined with the same swept-pump signal ("unlock") in a second stage FWM2, spatial information. A sample undergoing imaging can reflect idler signals at different times, based at least in part on distances of scattering layers, such as, for example, d_1 and d_2. Reflected or scattered optical signals incident at FWM2 can be converted to wavelength information.

[0023] Referring again to Figures 1(a) and 1(b), a corresponding temporal ray diagram is shown, where a two-stage FWM can be treated as a pair of converging and diverging time-lenses having identical focal length. The temporal ray diagrams show the WET principle, based on the space-time duality. When a converging lens is synchronized with the diverging lens, as shown in Figure 1(a), an output beam may continue to be along the same direction. If there is a temporal mismatch (Δt_d) between the converging lens and the diverging lens, as shown in Figure 1(b) an output beam may be redirected along a certain axial angle, which may comprise a different output wavelength.

[0024] In accordance with the principle of the space-time duality, the axial angle (or exit angle) may refer to the wavelength and the vertical direction refers to the time axis. Thus, spatial depth induced time delay (Δt_d) may result in vertical movement of the second time-lens, and may further convert a parallel beam comprising exit angle ($\theta=\Delta t_d/\varphi_f$), that is, a different wavelength in this temporal ray diagram. This mechanism can provides a linear relation between the reflection depth (d), such as d_1 and d_2 shown in Figures 1(c) and 1(d), and the output wavelength shift ($\Delta\lambda$), which can be expressed as follows:

$$\Delta\lambda = \frac{4d}{cDL} \qquad (3),$$

where c is the speed of light, D is the swept pump dispersion, and L is the dispersive fiber length. From Equation (3), it can be seen that the mapping ratio between depth and wavelength can be easily adjusted by controlling the pump dispersion (D).

[0025] Figure 6 shows a schematic diagram of a WET system according to an embodiment of the subject invention. Referring to Figure 6, a swept pump can be generated from a short pulsed source that may pass through a dispersive fiber. An output signal from the swept pump can be separated into two branches, for example, as the pump for the two-stage FWM, such as FWM1 and FWM2 (of Figures 1(c) and 1(d). In the first-stage FWM, the CW signal having a frequency f_{cw} and the swept pump generate the idler with doubled swept range. The idler can be separated and utilized to illuminate a sample (e.g., a sample under test). Different reflective depths of the sample can give rise to scattering of the idler signal proportional to temporal delay brought about by distances of layers of a sample undergoing imaging.

[0026] In certain examples, an optical delay line in a sample arm can assist in synchronizing scattered idlers with the second stage pump. Thus, a new idler generated at a frequency f_{cw} can form a signal comprising a spectrum based at least in part on geometrical profiles of features of layers comprising the sample undergoing imaging. In the time-lens system of Figure 6, a converging and diverging time-lens can be capable of performing in FWM stages, so long as an FWM combines with a signal side and another FWM combines with an idler side. Thus, in examples, the two- stage FWM configuration can be simplified to comprise a bidirectional FWM structure, as shown in Figure 7.

[0027] To rapidly capture a signal comprising a spectrum based at least in part on geometrical profiles of features of layers comprising the sample undergoing imaging, similar to the OCT system, a single frame detection may be capable of obtaining depth information of a single illumination point. Thus, referring again to Figure 5, to capture a 2-dimensional cross-section of an image, for example, a scanning mirror galvanometer (**M1**) can be used in the sample arm as shown in the left box of Figure 5.

[0028] In Figure 5(a), which may be used to illustrate a first of two methods, dispersing a spectrum of an output signal from a sample under test onto a spatial CCD sensor can be seen. A second scanning mirror galvanometer (**M2**) can be utilized, for example, to construct two-dimensional images. Scanning mirror galvanometer **M1** and **M2** can be synchronized by utilizing a driving signal that may be derived from a single source, for example. In general, the method illustrated in Figure 5(a) may be simpler and more straightforward than related art approaches, and may consume very few processing resources, or, in some instances, may require no post processing resources. However, the method illustrated in Figure 5(a) may be limited by a frame rate capacity of the charge coupled device (CCD) sensor, which may be capable of capturing, for example, thousands of frames per second. In contrast, implementations of WET systems can capture millions or billions of frames per second.

[0029] Referring again to Figure 5(b), in a second method, an optical spectrum analyzer, such as a PASTA, can be employed. In one instance, if a PASTA is utilized to synchronize a pump of the WET system, imaging information can be taken at, for example, every frame. By obtaining
imaging information with each frame, single-shot and/or single-frame imaging, as shown in Figure 5(b), can be attained.

[0030] According to many embodiments, a WET system can be employed and can be an optical imaging modality capable of capturing tomographic layered images in a non-invasive manner, and enabling ultrafast frame rates with high resolution and sensitivity. In related art techniques, if a continuous wave source is directly reflected from a sample undergoing imaging, it may be difficult to differentiate depth-induced delay of energy scattering from a sample undergoing testing. In many embodiments of the subject invention, a linear frequency shifted device (e.g., a time-lens) can be introduced in front of the sample undergoing imaging. As light or other optical energy transmits forward and backward through the WET system, the spectrum may be stretched and compressed. At the sample site, since illuminating energy may be a swept source, different reflecting depth may result in different output wavelengths after a compression process, thus realizing the separation of different layers. Certain aspects of a WET system may function similarly to those of an OCT technique, which relies on electrical Fourier transformation of the interference fringes.

[0031] While there may be little or no interference in the WET process, the device can bring about optical Fourier transform for the optical field, which improves the resolution by a factor of approximately 2 compared with the electrical Fourier transform when using a related art OCT technique. Considering the idler has doubled bandwidth of the pump, it improves the resolution by another factor of approximately 2. Therefore, under the same spectral bandwidth, a WET system can achieve up to 4 times sharper resolution than a related art OCT technique. Since some ultrafast spectro-temporal analyzers based on the time-lens focusing mechanism are available, a WET system can bring about single-shot imaging and provide orders of magnitude improvement in an imaging frame rate, which can be as high as millions or even billions of frames per second.

[0032] Advantages of WET versus OCT include, but are not necessarily limited to: (1) no separated reference branch is required in generating the interference pattern (fringes); (2) since the reference branch is not required, the imaging speed is not limited by the mechanical component (such as moving the reference arm in time-domain OCT to generate the fringes); (3) it is a predominantly ultrafast all-optical process, since the output scattered signal directly reflects the spatial information, and no post-processing is required compared with SD-OCT; (4) the WET system can, in principle, achieve four times sharper resolution than the OCT system with the same spectral bandwidth. Therefore, a WET system improves the A-scan rate and the imaging quality, and also largely simplifies system requirement.

[0033] Following are examples that illustrate procedures for practicing the invention. These examples should not be construed as limiting. All percentages are by weight and all solvent mixture proportions are by volume unless otherwise noted.

EXAMPLE 1

[0034] The performance of a WET system as shown in Figure 2 was evaluated. According to Equation (1), the output wavelength shift ($\Delta\lambda$) is directly proportional to the reflection depth (d). To quantitatively characterize this feature, a precision translation stage was be introduced to control the reflective mirror, which was moved with 1.25-mm separation across 11-mm range, and the results are shown in Figure 4. It was observed that the 3-dB observation range was up to 1 cm and the depth-to-wavelength mapping ratio was ε = 0.8 nm/mm, which matched well with Equation (1). In the WET system, the spatial resolution (R_{WET}) refers to the capability of an optical imaging system to distinguish different layers, which can be calculated with the spectral width ($\delta\lambda$) and the mapping ratio (ε). The ideal $\delta\lambda$ is determined by the temporal pulsewidth ($\lambda_{BW}DL$), which can be narrowed by the FWM process. It was noted that $\delta\lambda$ can be limited by the high frequency intensity fluctuation of the swept-pump. If there is no intensity fluctuation over the envelope of the swept-pump, and phase-matching condition is satisfied over the whole conversion range, and the spatial resolution of the WET system can be shown as Equation (2).

[0035] Based on the experimental pump bandwidth (λ_{BW} = 7.5 nm), the ideal spatial resolution should be 36 μm. Compared with OCT, the WET system can, in principle, achieve four times sharper resolution with the same bandwidth (λ_{BW}) based on Equation (2). The spectra of these two-stage FWMs are shown in Figure 3, and it is noted that the idler (**I1**) bandwidth (10 nm) was not ideally doubled compared to that of the swept-pump (7.5 nm), owing to the higher-order dispersion induced phase mismatch. Therefore, the conversion bandwidth also limited the resolution, and the phase matching condition requires shorter HNL-DSF with lower dispersion
coefficient (D) and slope (S). Some advanced dispersion-engineered nonlinear medium, such as a silicon waveguide, helps to achieve 100-nm FWM wavelength conversion bandwidth, which can benefit the implementation of the WET system. The inset of Figure 3(b) shows the comparison between the input and the output spectra, which was broadened from 0.05 nm (OSA resolution) to $\delta\lambda$ = 0.12 nm. Two factors contribute to this spectral broadening effect: first, the phase-mismatching decreased the pulsewidth of idler (**I1**) by 30%, since its bandwidth was degraded from 15 nm to 10 nm after FWM1 (as shown in Figure 3(a)). Considering the same narrowing effect in FWM2, the pulsewidth of idler (**I2**) may

decrease by half, i.e., broaden the spectral width by a factor of two (from 0.03 nm to 0.06 nm). Second, the temporal intensity fluctuation of the swept-pump introduced another factor of two to the spectral width of the idler (**I2**) from 0.06 nm to 0.12 nm. According to the measurement in Figure 4 (based on the OSA with 5-Hz frame rate), the corresponding resolution of the WET system evaluated was $R_{WET} = \delta\lambda/\varepsilon = 150$ μm, which is less than the ideal case given in Equation (2).

EXAMPLE 2

[0036] With ultrafast spectral acquisition modalities, the WET system of Example 1 was compared with a related art OCT system, and the results are shown in Table 1. The systems were compared using the same spectral bandwidth (7.5 nm), and the WET system achieved the same resolution as the OCT system, even with the degradation compared to the ideal case given in Equation (2).

[0037] Referring to Table 1, over 100 nm was available as a spectral width for OCT, and it can be an incoherent source in SD-OCT, Fourier domain mode-locking (FDML) laser source, or a semiconductor swept-source with micro-electro-mechanical mirror systems (MEMS) based filter in swept-source OCT. The spectral source in the WET system in this example could have been up to 10 nm, which was limited by the phase-matching condition of the FWM waveguide. The value listed for "Measured *R*" for the OCT is an estimated value, owing to the small resolution degradation introduced by the OCT system. The A-scan rate of the OCT was limited by the graphics processing unit processing speed (to perform the calibration and Fourier transform) in the SD-OCT.

Table 1. Comparison between OCT and WET system under the same spectral width (7.5 nm)

	OCT	**WET**
Spectral width (λ_{BW})	7.5 mm	7.5 mm
Resolution (*R*)	$R_{OCT} = 2\ln 2\lambda_0^2/(\pi\lambda_{BW})$	$R_{WET} = \ln 2\lambda_0^2/(2\pi\lambda_{BW})$
Theoretic *R*	144 μm	36 μm
Measured *R*	150 μm	150 μm
Depth range	> 1 cm	> 1 cm
A-scan rate (f_A)	40kHz	100 MHz

[0038] The spectral width of the WET system can be narrowed by extending the conversion bandwidth and/or reducing the intensity fluctuation of the swept-pump. Therefore, a more stable swept-pump can lead to a narrower spectral width.

[0039] It should be understood that the examples and embodiments described herein are for illustrative purposes only and that various modifications or changes in light thereof will be suggested to persons skilled in the art and are to be included within the scope of the appended claims.

REFERENCES

[0040]

A. M. Zysk, F. T. Nguyen, A. L. Oldenburg, D. L. Marks, and S. A. Boppart, "Optical coherence tomography: A review of clinical development from bench to bedside," J. Biomed. Opt., 12, 051403 (2007).

D. Huang, E. A. Swanson, C. P. Lin, J. S. Schuman, W. G Stinson, W. Chang, M. R. Hee, T. Flotte, K. Gregory, C. A. Puliafito, and J. G Fujimoto, "Optical coherence tomography," Science, 254 (5035) 1178-1181 (1991).

S. Yun, G Tearney, J. de Boer, N. Iftimia, and B. Bouma, "High-speed optical frequency-domain imaging," Opt. Exp., 11, 29532963 (2003).

R. A. Leitgeb, W. Drexler, A. Unterhuber, B. Hermann, T. Bajraszewski, T. Le, A. Stingl, and A. F. Fercher, "Ultrahigh resolution Fourier domain optical coherence tomography," Opt. Lett., 12, 2156-2158 (2004).

G. N. Hounsfield, "Computerized transverse axial scanning (tomography): Part I. Description of system," Br. J. Radiol 46, 1016-1022 (1973).

R. Damadian, M. Goldsmith, and L. Minkoff, "NMR in Cancer: XVI. FONAR image of the live human body," Physiol.

Chem. Phys. 9, 97-100 (1977).

J. J. Wild and J. M. Reid, "Application of echo-ranging techniques to the determination of structure of biological tissues," Science 115, 226-230 (1952).

D. Huang, E. A. Swanson, C. P. Lin, J. S. Schuman, W. G. Stinson, W. Chang, M. R. Hee, T. Flotte, K. Gregory, C. A. Puliafito, and J. G. Fujimoto, "Optical coherence tomography," Science 254, 1178-1181 (1991).

W. Wieser, B. R. Biedermann, T. Klein, C. M. Eigenwillig, and R. Huber, "Multi-Megahertz OCT: High quality 3D imaging at 20 million A-scans and 4.5 GVoxels per second," Opt. Express 18, 14685-14704 (2010).

B. Chance, J. S. Leigh, H. Miyake, D. S. Smiths, S. Nioka, R. Greenfeld, M. Finander, K. Kaufmann, W. Levy, M. Young, P. Cohen, H. Yoshioka, and R. Boretsky, "Comparison of time-resolved and -unresolved measurements of deoxyhemoglobin in brain," Proc. Natl. Acad. Sci. USA 85, 4971-4975 (1988).

M. A. Foster, R. Salem, D. F. Geraghty, A. C. Turner-Foster, M. Lipson, and A. L. Gaeta, "Silicon-chip-based ultrafast optical oscilloscope," Nature 456, 81-84 (2008).

B. H. Kolner, "Space-time duality and the theory of temporal imaging," IEEE J. Quantum Electron. 30, 1951-1963 (1994).

A. E. Conrady, Applied Optics and Optical Design, Part One (Courier Dover Publications, 2011).

C. Zhang, K. K. Y. Cheung, P. C. Chui, K. K. Tsia, and K. K. Y. Wong, "Fiber optical parametric amplifier with high-speed swept pump," IEEE Photonics. Technol. Lett. 23, 1022-1024 (2011).

C. Zhang, P. C. Chui, and K. K. Y. Wong, "Comparison of state-of-art phase modulators and parametric mixers in time-lens applications under different repetition rates," Appl. Opt. 52, 8817-8826 (2013).

M. E. Marhic, Fiber Optical Parametric Amplifiers, Oscillators and Related Devices (Cambridge University Press, Cambridge, 2007).

A. C. Turner-Foster, M. A. Foster, R. Salem, A. L. Gaeta, and M. Lipson, "Frequency conversion over two-thirds of an octave in silicon nano-waveguides," Opt. Express 18, 1904-1908 (2010).

S. Yun, G. Tearney, J. de Boer, N. Iftimia, and B. Bouma, "High-speed optical frequency-domain imaging," Opt. Express 11, 2953-2963 (2003).

R. A. Leitgeb, W. Drexler, A. Unterhuber, B. Hermann, T. Bajraszewski, T. Le, A. Stingl, and A. F. Fercher, "Ultrahigh resolution Fourier domain optical coherence tomography," Opt. Lett. 12, 2156-2158 (2004).

D. R. Solli, J. Chou, and B. Jalali, "Amplified wavelength-time transformation for real-time spectroscopy," Nat. Photonics 2, 48-51 (2008).

C. Zhang, J. Xu, P. C. Chui, and K. K. Y. Wong, "Parametric spectro-temporal analyzer (PASTA) for real-time optical spectrum observation," Sci. Rep. 3, 2064 (2013).

T. G. Etoh, C. V. Le, Y. Hashishin, N. Otsuka, K. Takehara, H. Ohtake, T. Hayashida, and H. Maruyama, "Evolution of Ultra-High-Speed CCD Imagers," Plasma Fusion Res. 2, S1021 (2007).

C. Zhang, X. Wei, and K. K. Y. Wong, "Performance of parametric spectro-temporal analyzer (PASTA)," Opt. Express 21, 32111-32122 (2013).

R. Huber, M. Wojtkowski, and J. G. Fujimoto, "Fourier domain mode locking (FDML): A new laser operating regime and applications for optical coherence tomography," Opt. Express 14, 3225-3237 (2006).

Claims

1. A tomographic imaging system, comprising:

   a sample platform;
   a photodetector;
   a linear frequency-shifted device comprising two time-lenses configured to have opposite focal group-dispersion delays from each other and positioned such that light passes through a first of the time-lenses before illuminating a sample on the sample platform and such that light from the sample passes through a second of the time-lenses before it reaches the photodetector; and
   a processing device in operable communication with the photodetector and configured to receive an output spectrum from the photodetector,
   wherein the imaging system is configured to realize an all-optical spatial to wavelength conversion with a flexible conversion factor.

2. The tomographic imaging system according to claim 1, wherein the processing device is an optical spectrum analyzer.

3. The tomographic imaging system according to claim 1, further comprising a swept-pump, a first four-wave mixer FWM in operable communication with the swept-pump, and a second FWM in operable communication with the swept-pump.

4. The tomographic imaging system according to claim 3, wherein the first FWM is a highly-nonlinear dispersion-shifted fiber HNL-DSF and wherein the second FWM is an HNL-DSF.

5. The tomographic imaging system according to claim 1, wherein the processing device comprises a parametric spectro-temporal analyzer PASTA.

6. The tomographic imaging system according to claim 1, wherein the system is capable of achieving an imaging resolution of 150 μm or less with a spectral width of 7.5 nm.

7. The tomographic imaging system according to claim 6, wherein the system is capable of achieving an A-scan rate of at least 100 MHz.

8. A method for imaging capturing a tomographic image of a sample, the method comprising:

   placing the sample on a sample platform of an imaging system;
   positioning a linear frequency-shifted device that comprises two time-lenses configured to have opposite focal group-dispersion delays from each other such that light passes through a first of the time-lenses before illuminating the sample and such that light from the sample passes through a second of the time-lenses before it reaches a photodetector of the imaging system; and
   receiving, by a processing device in operable communication with the photodetector, an output spectrum from the photodetector,
   wherein the imaging system realizes an all-optical spatial to wavelength conversion with a flexible conversion factor.

9. The method according to claim 8, wherein the processing device is an optical spectrum analyzer.

10. The method according to claim 8, wherein the imaging system further comprises a swept-pump, a first four-wave mixer FWM in operable communication with the swept-pump, and a second FWM in operable communication with the swept-pump, and
    wherein the first FWM provides a signal to the sample platform.

11. The method according to claim 10, wherein the first four-wave mixer is a highly-nonlinear dispersion-shifted fiber, and wherein the second four-wave mixer is an highly-nonlinear dispersion-shifted fiber.

12. The method according to claim 8, wherein the processing device comprises a parametric spectro-temporal analyzer PASTA.

13. The method according to claim 9, wherein the method achieves an imaging resolution of 150 μm or less with a spectral width of 7.5 nm.

14. The method according to claim 9, wherein the method achieves an A-scan rate of at least 100 MHz.

Patentansprüche

1. Bildgebendes Tomografiesystem, umfassend:

   eine Probenplattfom;
   einen Photodetektor;
   eine Vorrichtung mit linearer Frequenzverschiebung, die zwei Zeitlinsen umfasst, die so gestaltet sind, dass sie entgegengesetzte Fokusgruppen-Dispersionsverzögerungen zueinander aufweisen und so positioniert sind, dass Licht durch eine erste der Zeitlinsen tritt, bevor es eine Probe auf der Probenplattform illuminiert und so, dass Licht von der Probe durch eine zweite der Zeitlinsen tritt, bevor es den Photodetektor erreicht; und
   eine Verarbeitungsvorrichtung in betriebsfähiger Kommunikation mit dem Photodetektor und so gestaltet, dass sie ein Ausgangsspektrum von dem Photodetektor empfängt,
   wobei das bildgebende System so gestaltet ist, dass es eine rein optische Raum-Wellenlängen-Umwandlung mit einem flexiblen Umwandlungsfaktor realisiert.

2. Bildgebendes Tomografiesystem nach Anspruch 1, wobei die Verarbeitungsvorrichtung ein optischer Spektrumanalysator ist.

3. Bildgebendes Tomografiesystem nach Anspruch 1, ferner umfassend eine Swept-Pumpe, einen ersten Vierwellen-Mischer, FWM, in betriebsfähiger Kommunikation mit der Swept-Pumpe, und einen zweiten FWM in betriebsfähiger Kommunikation mit der Swept-Pumpe.

4. Bildgebendes Tomografiesystem nach Anspruch 3, wobei der erste FWM eine höchst nichtlineare dispersionsverschobene Faser, HNL-DSF, ist, und wobei der zweite FWM eine HNL-DSF ist.

5. Bildgebendes Tomografiesystem nach Anspruch 1, wobei die Verarbeitungsvorrichtung einen parametrischen spektro-zeitlichen Analysator, PASTA, umfasst.

6. Bildgebendes Tomografiesystem nach Anspruch 1, wobei das System eine bildgebende Auflösung von 150 μm oder weniger mit eine Spektralbreite von 7,5 mm erreichen kann.

7. Bildgebendes Tomografiesystem nach Anspruch 6, wobei das System eine A-Scanrate von mindestens 100 MHz erreichen kann.

8. Verfahren zur Bilderfassung eines tomografischen Bilds einer Probe, wobei das Verfahren folgendes umfasst:

   Platzieren der Probe auf einer Probenplattform eines bildgebenden Systems;
   Positionieren einer Vorrichtung mit linearer Frequenzverschiebung, die zwei Zeitlinsen umfasst, die so gestaltet sind, dass sie entgegengesetzte Fokusgruppen-Dispersionsverzögerungen zueinander aufweisen und so, dass Licht durch eine erste der Zeitlinsen tritt, bevor es eine Probe auf der Probenplattform illuminiert, und so, dass Licht von der Probe durch eine zweite der Zeitlinsen tritt, bevor es den Photodetektor erreicht; und
   Empfangen eines Ausgangsspektrums von dem Photodetektor durch eine Verarbeitungsvorrichtung in betriebsfähiger Kommunikation mit dem Photodetektor; und
   wobei das bildgebende System eine rein optische Raum-Wellenlängen-Umwandlung mit einem flexiblen Umwandlungsfaktor realisiert.

9. Verfahren nach Anspruch 8, wobei die Verarbeitungsvorrichtung ein optischer Spektrumanalysator ist.

10. Verfahren nach Anspruch 8, wobei das bildgebende System ferner eine Swept-Pumpe, einen ersten Vierwellen-Mischer, FWM, in betriebsfähiger Kommunikation mit der Swept-Pumpe, und einen zweiten FWM in betriebsfähiger Kommunikation mit der Swept-Pumpe umfasst, und wobei
    der erste FWM ein Signal an die Probenplattform bereitstellt.

11. Verfahren nach Anspruch 10, wobei der erste Vierwellen-Mischer eine höchst nichtlineare dispersionsverschobene Faser ist, und wobei der zweite Vierwellen-Mischer eine höchst nichtlineare dispersionsverschobene Faser ist.

12. Verfahren nach Anspruch 8, wobei die Verarbeitungsvorrichtung einen parametrischen spektro-zeitlichen Analysator, PASTA, umfasst.

13. Verfahren nach Anspruch 9, wobei das System eine bildgebende Auflösung von 150 μm oder weniger mit eine Spektralbreite von 7,5 mm erreicht.

14. Verfahren nach Anspruch 9, wobei das System eine A-Scanrate von mindestens 100 MHz erreicht.

Revendications

1. Système d'imagerie tomographique, comprenant :

   une plate-forme d'échantillonnage ;
   un photodétecteur ;
   un dispositif à fréquence décalée linéaire comprenant deux lentilles temporelles conçues pour présenter des délais opposés de groupe focal-dispersion l'une par rapport à l'autre et positionnées de sorte que la lumière passe à travers une première des lentilles temporelles avant d'illuminer un échantillon sur la plate-forme d'échantillonnage et de sorte que la lumière de l'échantillon passe à travers une seconde des lentilles temporelles avant d'atteindre le photodétecteur ; et
   un dispositif de traitement en communication fonctionnelle avec le photodétecteur et conçu pour recevoir un spectre de sortie photodétecteur,
   dans lequel le système d'imagerie est conçu pour réaliser une conversion toute optique spatiale à longueur d'onde avec un facteur de conversion flexible.

2. Système d'imagerie tomographique selon la revendication 1, dans lequel le dispositif de traitement est un analyseur de spectre optique.

3. Système d'imagerie tomographique selon la revendication 1, comprenant en outre une pompe à balayage, un premier mélangeur FWM à quatre ondes en communication fonctionnelle avec la pompe à balayage, et un second FWM en communication fonctionnelle avec la pompe à balayage.

4. Système d'imagerie tomographique selon la revendication 3, dans lequel le premier FWM est une fibre à dispersion décalée hautement non linéaire HNL-DSF et dans lequel le second FWM est un HNL-DSF.

5. Système d'imagerie tomographique selon la revendication 1, dans lequel le dispositif de traitement comprend un analyseur PASTA spectro-temporel paramétrique.

6. Système d'imagerie tomographique selon la revendication 1, dans lequel le système est capable d'obtenir une résolution d'image inférieure ou égale à 150 μm avec une largeur spectrale de 7,5 nm.

7. Système d'imagerie tomographique selon la revendication 6, dans lequel le système est capable d'obtenir un taux de balayage A d'au moins 100 MHz.

8. Procédé destiné à la capture d'image d'une image tomographique d'un échantillon, le procédé comprenant :

   le placement de l'échantillon sur une plate-forme d'échantillonnage d'un système d'imagerie ;
   le positionnement d'un dispositif à fréquence décalée linéaire qui comprend deux lentilles temporelles conçues pour présenter des délais opposés de groupe focal-dispersion l'une par rapport à l'autre de sorte que la lumière passe à travers une première des lentilles temporelles avant d'illuminer l'échantillon et de sorte que la lumière provenant de l'échantillon passe à travers une seconde des lentilles temporelles avant d'atteindre un photodétecteur du système d'imagerie ; et
   la réception, au moyen d'un dispositif de traitement en communication fonctionnelle avec le photodétecteur, d'un spectre de sortie provenant du photodétecteur,
   dans lequel le système d'imagerie réalise une conversion toute optique spatiale à longueur d'onde avec un

facteur de conversion flexible.

9. Procédé selon la revendication 8, dans lequel le dispositif de traitement est un analyseur de spectre optique.

10. Procédé selon la revendication 8, dans lequel le système d'imagerie comprend en outre une pompe à balayage, un premier mélangeur FWM à quatre ondes en communication fonctionnelle avec la pompe à balayage, et un second FWM en communication fonctionnelle avec la pompe à balayage.

11. Procédé selon la revendication 10, dans lequel le premier mélangeur à quatre ondes est une fibre à dispersion décalée hautement non linéaire, dans lequel le second mélangeur à quatre ondes est une fibre à dispersion décalée hautement non linéaire.

12. Procédé selon la revendication 8, dans lequel le dispositif de traitement comprend un analyseur PASTA spectro-temporel paramétrique.

13. Procédé selon la revendication 9, dans lequel le procédé réalise une résolution d'image inférieure ou égale à 150 μm avec une largeur spectrale de 7,5 nm.

14. Procédé selon la revendication 9, dans lequel le procédé réalise un taux de balayage A d'au moins 100 MHz.

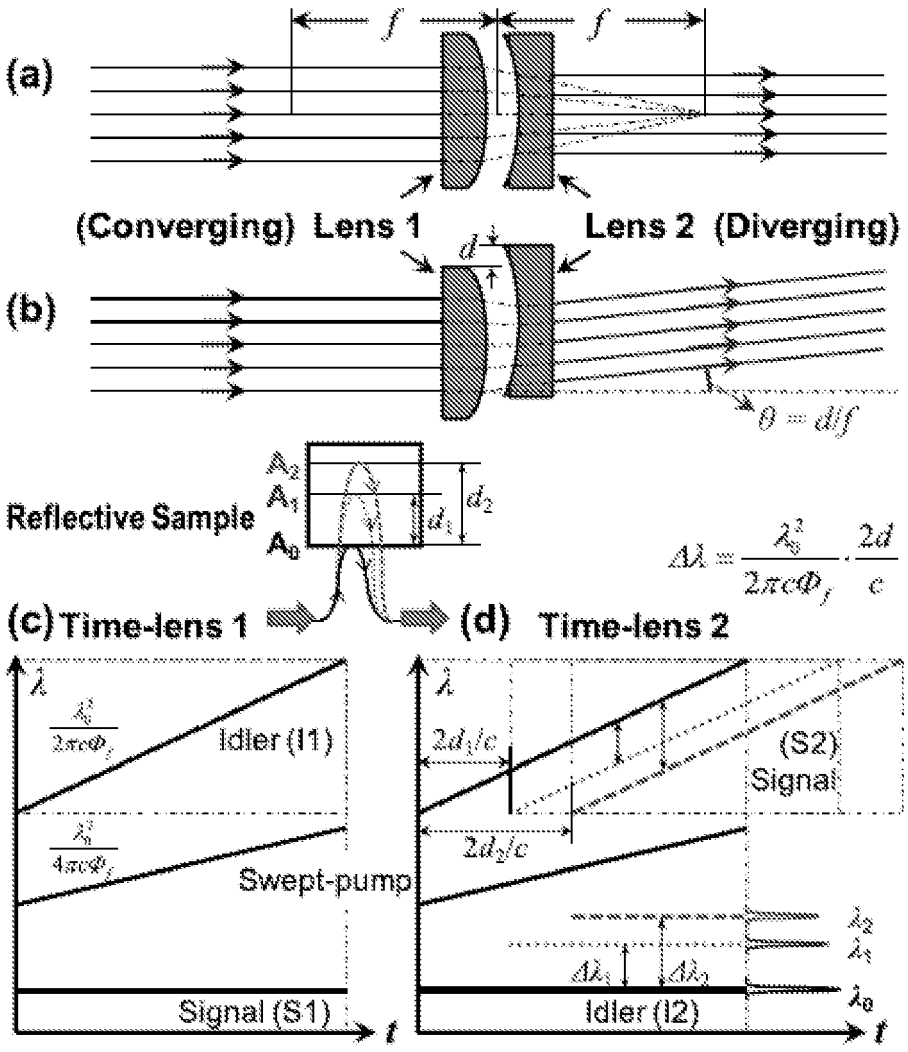
(a)
f
f
(Converging) Lens 1
Lens 2 (Diverging)
(b)
d
θ = d/f
Reflective Sample
A2
A1
A0
d2
d1
(c) Time-lens 1
(d) Time-lens 2
Idler (I1)
Swept-pump
Signal (S1)
(S2) Signal
Idler (I2)
2d1/c
2d2/c
λ2
λ1
λ0
t

FIG. 1

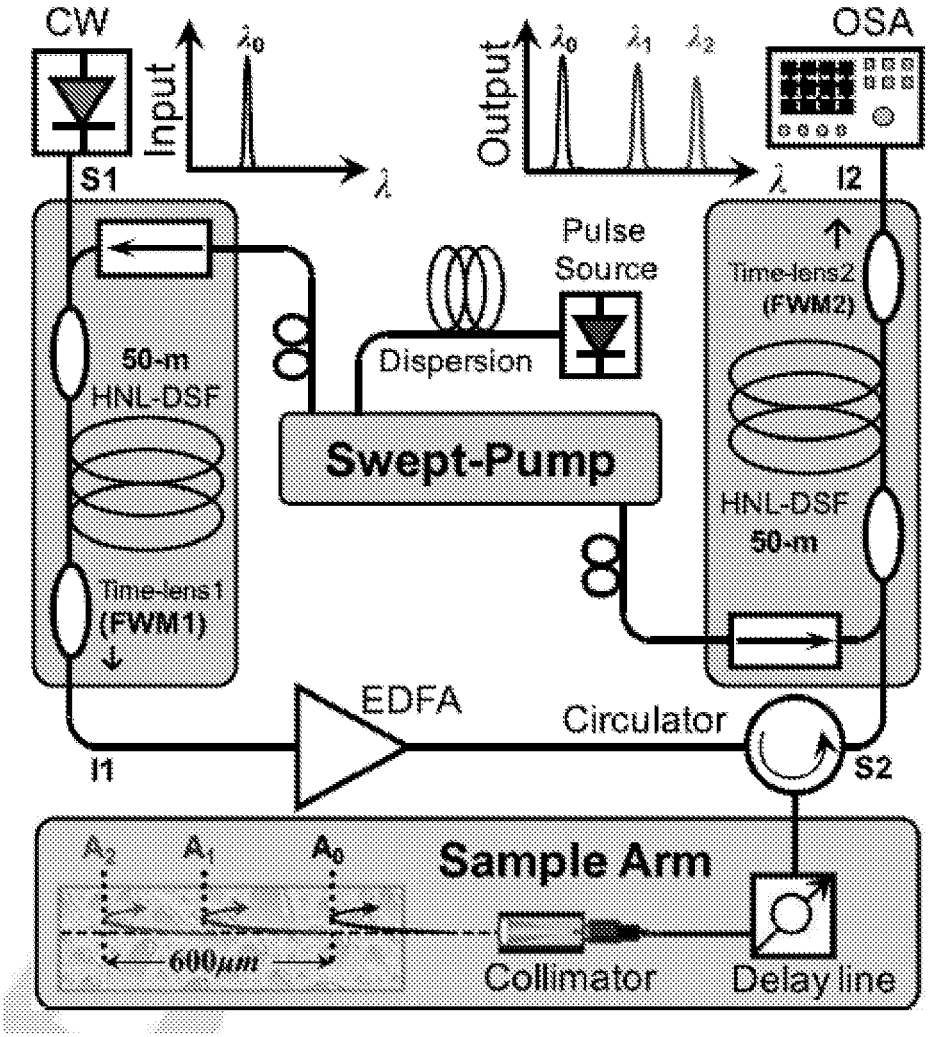
CW
Input
λ_0
λ
S1
Output
λ_0
λ_1
λ_2
OSA
λ
I2
Pulse
Source
Dispersion
Time-lens2
(FWM2)
50-m
HNL-DSF
Swept-Pump
HNL-DSF
50-m
Time-lens1
(FWM1)
EDFA
Circulator
I1
S2
A_2
A_1
A_0
Sample Arm
600μm
Collimator
Delay line

FIG. 2

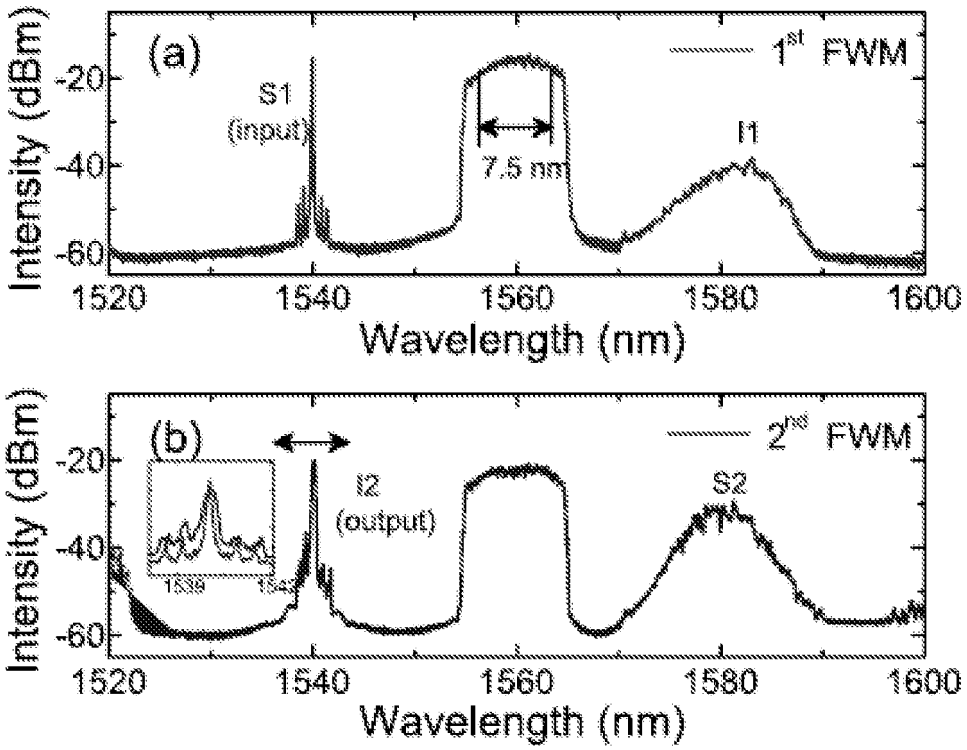
(a)
1st FWM
S1
(input)
7.5 nm
I1
Intensity (dBm)
-20
-40
-60
1520
1540
1560
1580
1600
Wavelength (nm)
(b)
2nd FWM
I2
(output)
S2
Intensity (dBm)
-20
-40
-60
1520
1540
1560
1580
1600
Wavelength (nm)

FIG. 3

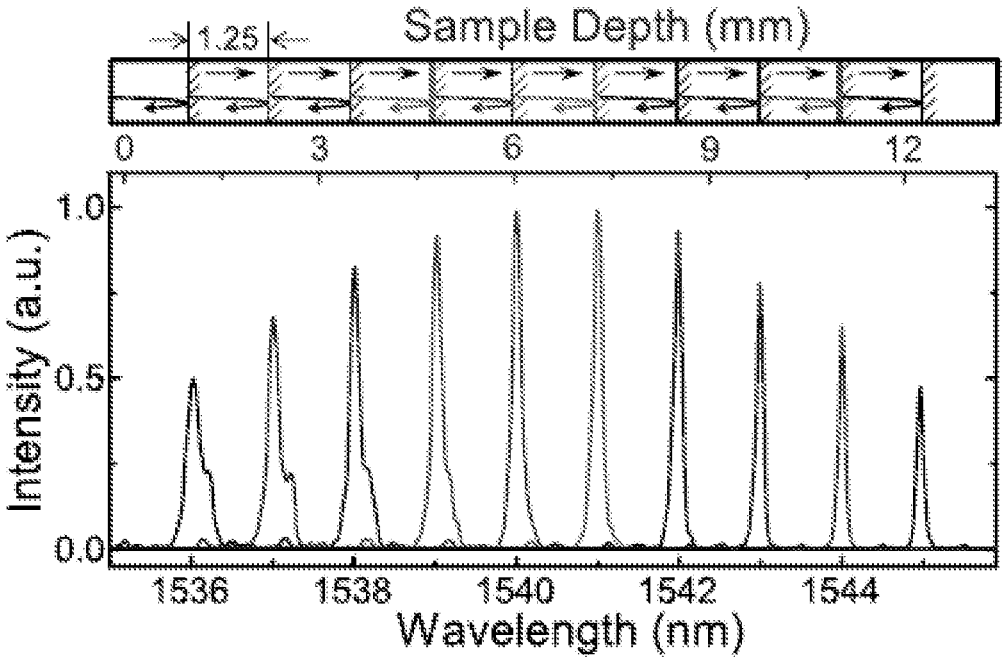
Sample Depth (mm)
1.25
0
3
6
9
12
Intensity (a.u.)
1.0
0.5
0.0
1536
1538
1540
1542
1544
Wavelength (nm)

FIG. 4

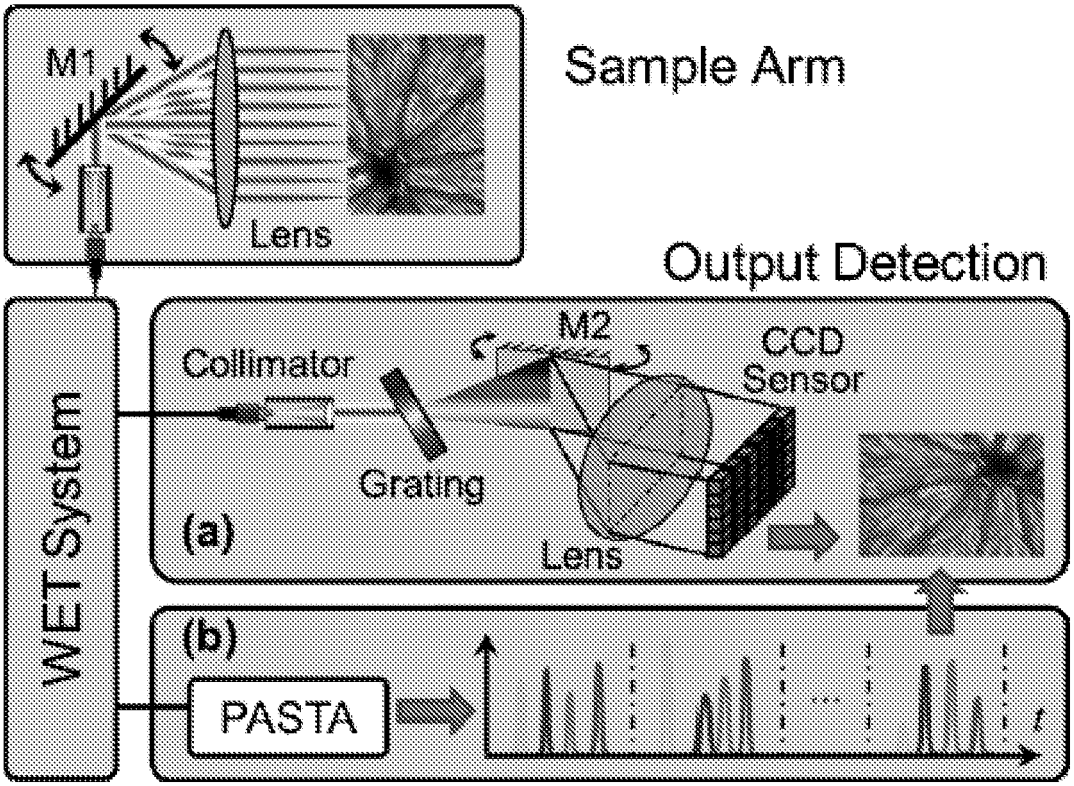
M1
Lens
Sample Arm
Output Detection
WET System
Collimator
M2
CCD
Sensor
Grating
(a)
Lens
(b)
PASTA
t

FIG. 5

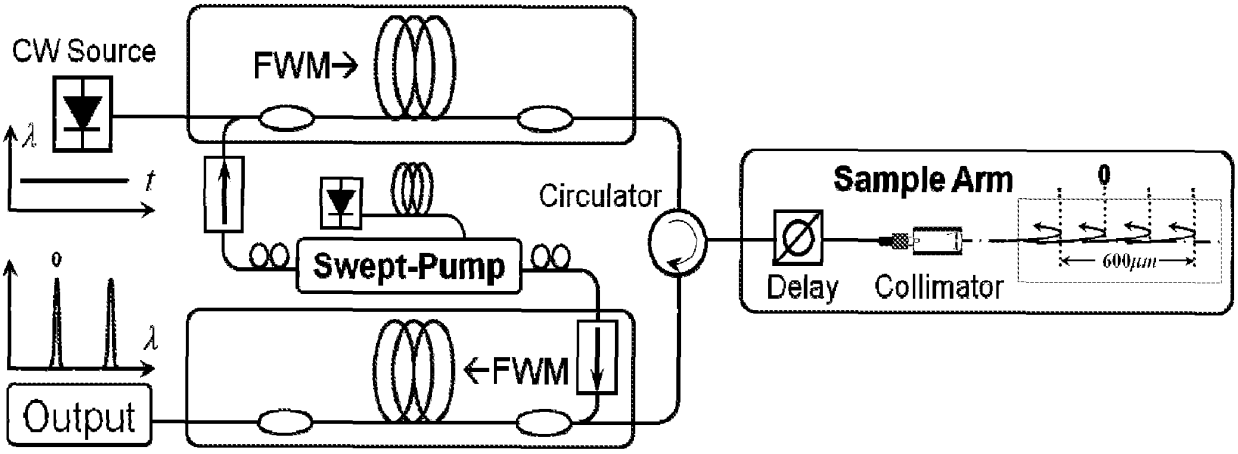
CW Source
FWM→
λ
t
Circulator
Sample Arm
0
Swept-Pump
Delay
Collimator
600μm
0
λ
←FWM
Output

FIG. 6

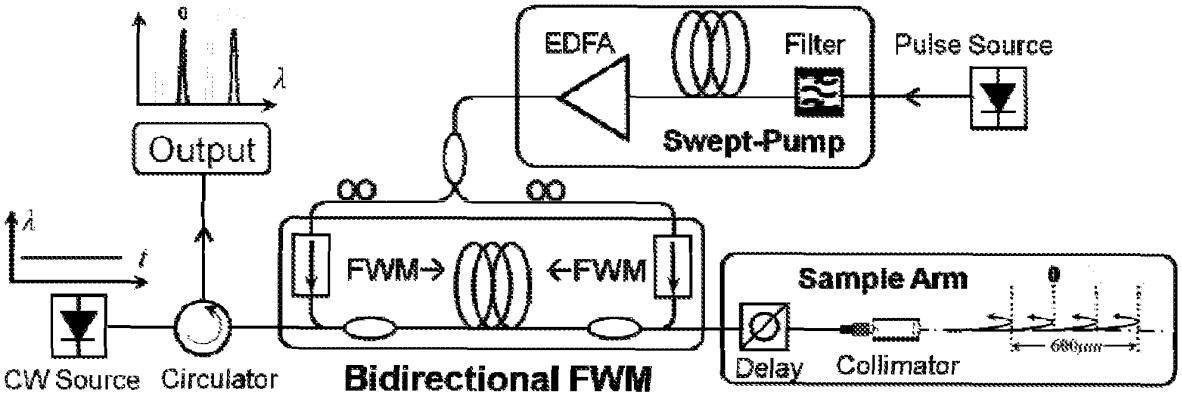
0
λ
EDFA
Filter
Pulse Source
Output
Swept-Pump
λ
t
FWM→
←FWM
Sample Arm
0
CW Source
Circulator
Bidirectional FWM
Delay
Collimator
680μm

FIG. 7

REFERENCES CITED IN THE DESCRIPTION

This list of references cited by the applicant is for the reader's convenience only. It does not form part of the European patent document. Even though great care has been taken in compiling the references, errors or omissions cannot be excluded and the EPO disclaims all liability in this regard.

Patent documents cited in the description

- CN 103284691 A **[0004]**

Non-patent literature cited in the description

- **ONUR KUZUCU et al.** Spectral phase conjugation via temporal imaging. *OPTICS EXPRESS,* 26 October 2009 **[0004]**
- **REZA SALEM et al.** Application of space-time duality to ultrahigh-speed optical signal processing. *ADVANCES IN OPTICS AND PHOTONICS,* 30 September 2013 **[0004]**
- **MOTI FRIDMAN et al.** Demonstration of temporal cloaking. *NATURE,* 05 January 2012 **[0004]**
- **ZHANG et al.** Parametric spectro-temporal analyzer (PASTA) for real-time optical spectrum observation. *SCIENTIFIC REPORTS,* 24 June 2013 **[0004]**
- Principles of parametric temporal imaging. I. System configurations. **BENNETT C V et al.** IEEE JOURNAL OF QUANTUM ELECTRONICS. IEEE SERVICE CENTER, 04 April 2000 **[0004]**
- **ZHANG et al.** *Appl. Opt.,* 2013, 8817-8826 **[0014]**
- **A. M. ZYSK ; F. T. NGUYEN ; A. L. OLDENBURG ; D. L. MARKS ; S. A. BOPPART.** Optical coherence tomography: A review of clinical development from bench to bedside. *J. Biomed. Opt.,* 2007, vol. 12, 051403 **[0040]**
- **D. HUANG ; E. A. SWANSON ; C. P. LIN ; J. S. SCHUMAN ; W. G STINSON ; W. CHANG ; M. R. HEE ; T. FLOTTE ; K. GREGORY ; C. A. PULIAFITO.** Optical coherence tomography. *Science,* 1991, vol. 254 (5035), 1178-1181 **[0040]**
- **S. YUN ; G TEARNEY ; J. DE BOER ; N. IFTIMIA ; B. BOUMA.** High-speed optical frequency-domain imaging. *Opt. Exp.,* 2003, vol. 11, 29532963 **[0040]**
- **R. A. LEITGEB ; W. DREXLER ; A. UNTERHUBER ; B. HERMANN ; T. BAJRASZEWSKI ; T. LE, A. STINGL ; A. F. FERCHER.** Ultrahigh resolution Fourier domain optical coherence tomography. *Opt. Lett.,* 2004, vol. 12, 2156-2158 **[0040]**
- **G. N. HOUNSFIELD.** Computerized transverse axial scanning (tomography): Part I. Description of system. *Br. J. Radiol,* 1973, vol. 46, 1016-1022 **[0040]**
- **R. DAMADIAN ; M. GOLDSMITH ; L. MINKOFF.** NMR in Cancer: XVI. FONAR image of the live human body. *Physiol. Chem. Phys.,* 1977, vol. 9, 97-100 **[0040]**
- **J. J. WILD ; J. M. REID.** Application of echo-ranging techniques to the determination of structure of biological tissues. *Science,* 1952, vol. 115, 226-230 **[0040]**
- **D. HUANG ; E. A. SWANSON ; C. P. LIN ; J. S. SCHUMAN ; W. G. STINSON ; W. CHANG ; M. R. HEE ; T. FLOTTE ; K. GREGORY ; C. A. PULIAFITO.** Optical coherence tomography. *Science,* 1991, vol. 254, 1178-1181 **[0040]**
- **W. WIESER ; B. R. BIEDERMANN ; T. KLEIN ; C. M. EIGENWILLIG ; R. HUBER.** Multi-Megahertz OCT: High quality 3D imaging at 20 million A-scans and 4.5 GVoxels per second. *Opt. Express,* 2010, vol. 18, 14685-14704 **[0040]**
- **B. CHANCE ; J. S. LEIGH ; H. MIYAKE ; D. S. SMITHS ; S. NIOKA ; R. GREENFELD ; M. FINANDER ; K. KAUFMANN ; W. LEVY ; M. YOUNG.** Comparison of time-resolved and -unresolved measurements of deoxyhemoglobin in brain. *Proc. Natl. Acad. Sci. USA,* 1988, vol. 85, 4971-4975 **[0040]**
- **M. A. FOSTER ; R. SALEM ; D. F. GERAGHTY ; A. C. TURNER-FOSTER ; M. LIPSON ; A. L. GAETA.** Silicon-chip-based ultrafast optical oscilloscope. *Nature,* 2008, vol. 456, 81-84 **[0040]**
- **B. H. KOLNER.** Space-time duality and the theory of temporal imaging. *IEEE J. Quantum Electron.,* 1994, vol. 30, 1951-1963 **[0040]**
- **A. E. CONRADY.** Applied Optics and Optical Design. Courier Dover Publications, 2011 **[0040]**
- **C. ZHANG ; K. K. Y. CHEUNG ; P. C. CHUI ; K. K. TSIA ; K. K. Y. WONG.** Fiber optical parametric amplifier with high-speed swept pump. *IEEE Photonics. Technol. Lett.,* 2011, vol. 23, 1022-1024 **[0040]**
- **C. ZHANG ; P. C. CHUI ; K. K. Y. WONG.** Comparison of state-of-art phase modulators and parametric mixers in time-lens applications under different repetition rates. *Appl. Opt.,* 2013, vol. 52 **[0040]**
- **M. E. MARHIC.** Fiber Optical Parametric Amplifiers, Oscillators and Related Devices. Cambridge University Press, 2007 **[0040]**

- **A. C. TURNER-FOSTER ; M. A. FOSTER ; R. SALEM ; A. L. GAETA ; M. LIPSON.** Frequency conversion over two-thirds of an octave in silicon nano-waveguides. *Opt. Express,* 2010, vol. 18, 1904-1908 **[0040]**
- **S. YUN ; G. TEARNEY ; J. DE BOER ; N. IFTIMIA ; B. BOUMA.** High-speed optical frequency-domain imaging. *Opt. Express,* 2003, vol. 11, 2953-2963 **[0040]**
- **R. A. LEITGEB ; W. DREXLER ; A. UNTERHUBER ; B. HERMANN ; T. BAJRASZEWSKI ; T. LE ; A. STINGL ; A. F. FERCHER.** Ultrahigh resolution Fourier domain optical coherence tomography. *Opt. Lett.,* 2004, vol. 12, 2156-2158 **[0040]**
- **D. R. SOLLI ; J. CHOU ; B. JALALI.** Amplified wavelength-time transformation for real-time spectroscopy. *Nat. Photonics,* 2008, vol. 2, 48-51 **[0040]**
- **C. ZHANG ; J. XU ; P. C. CHUI ; K. K. Y. WONG.** Parametric spectro-temporal analyzer (PASTA) for real-time optical spectrum observation. *Sci. Rep.,* 2013, vol. 3, 2064 **[0040]**
- **T. G. ETOH ; C. V. LE ; Y. HASHISHIN ; N. OTSUKA ; K. TAKEHARA ; H. OHTAKE ; T. HAYASHIDA ; H. MARUYAMA.** Evolution of Ultra-High-Speed CCD Imagers. *Plasma Fusion Res.,* 2007, vol. 2, S1021 **[0040]**
- **C. ZHANG ; X. WEI ; K. K. Y. WONG.** Performance of parametric spectro-temporal analyzer (PASTA). *Opt. Express,* 2013, vol. 21, 32111-32122 **[0040]**
- **R. HUBER ; M. WOJTKOWSKI ; J. G. FUJIMOTO.** Fourier domain mode locking (FDML): A new laser operating regime and applications for optical coherence tomography. *Opt. Express,* 2006, vol. 14, 3225-3237 **[0040]**